

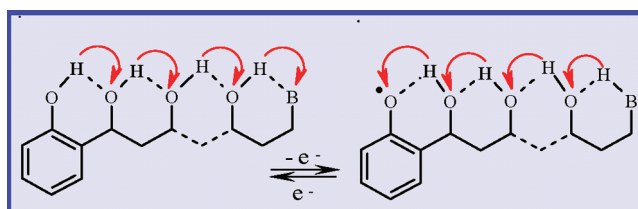
## Hydrogen-Bond Relays in Concerted Proton–Electron Transfers

JULIEN BONIN, CYRILLE COSTENTIN, MARC ROBERT,  
JEAN-MICHEL SAVÉANT,\* AND CÉDRIC TARD

*Université Paris Diderot, Sorbonne Paris Cité, Laboratoire d'Electrochimie  
Moléculaire, Unité Mixte de Recherche Univ - CNRS No 7591,  
Bâtiment Lavoisier, 15 rue Jean de Baïff, 75205 Paris Cedex 13, France*

RECEIVED ON MAY 8, 2011

### CONSPECTUS



**R**eaction mechanisms in which electron and proton transfers are coupled are central to a huge number of processes, both natural and synthetic. Moreover, most of the new approaches to address modern energy challenges involve proton-coupled electron transfer (PCET). Recent research has focused on the possibility that the two steps are concerted, that is, concerted proton–electron transfer (CPET) reactions, rather than stepwise pathways in which proton transfer precedes (PET) or follows (EPT) electron transfer. CPET pathways have the advantage of bypassing the high-energy intermediates of stepwise pathways, although this thermodynamic benefit may have a kinetic cost. Concerted processes require short distances between the group being oxidized and the proton acceptor (and vice versa for a reduction process), which usually involves the formation of a hydrogen bond. Unlike the electron in outer-sphere electron-transfer reactions, the distance a proton may travel in a CPET is therefore rather limited.

The idea has recently emerged, however, that this distance may be substantially increased via a H-bond relay located between the electron-transfer-triggered proton source and the proton acceptor. Generally speaking, the relay is a group bearing a H atom able to accept a H-bond from the moiety being oxidized and, at the same time, to form a H-bond with the proton-accepting group without going through a protonated intermediate. Although these molecules do not retain all the properties of chains of water molecules engaged in Grotthuss-type transport of a proton, the OH group in these molecules does possess a fundamental property of water molecules: namely, it is both a hydrogen-bond acceptor and a hydrogen-bond donor. Despite centuries of study, the mechanisms of proton movement in water remain active experimental and theoretical research areas, but so far with no connection to CPET reactions.

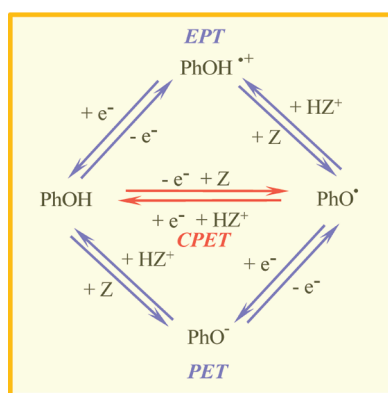
In this Account, we bring together recent results concerning (i) the oxidative response of molecules containing a H-bond relay and (ii) the oxidation of phenol with water (in water) as the proton acceptor. In the first case, a nondestructive electrochemical method (cyclic voltammetry) was used to investigate the oxidation of phenol molecules containing one H-bond relay and an amine proton acceptor compared with a similar amino phenol deprived of relay. In the second, the kinetics of phenol oxidation with water (in water) as proton acceptor is contrasted with that of conventional proton acceptors (such as hydrogen phosphate and pyridine) to afford evidence of the concerted nature of Grotthuss-type proton displacement with electron transfer. First indications were provided by the same electrochemical method, whereas a more complete kinetic characterization was obtained from laser flash photolysis. Older electrochemical results concerning the reduction of superoxide ion in the presence of water are also examined. The result is a timely picture of current insight into concerted mechanisms involving electron transfer coupled with proton transport over simple H-bond relays and over H-bond networks.

### Introduction

The coupling between electron transfer and proton transfer occurs in a huge number of natural and artificial processes.

Because they are involved in the electron transfer activation of small molecules, such as H<sub>2</sub>O, O<sub>2</sub>, and CO<sub>2</sub>,<sup>1,2</sup> the growing attention that these reactions attract is likely to be

SCHEME 1



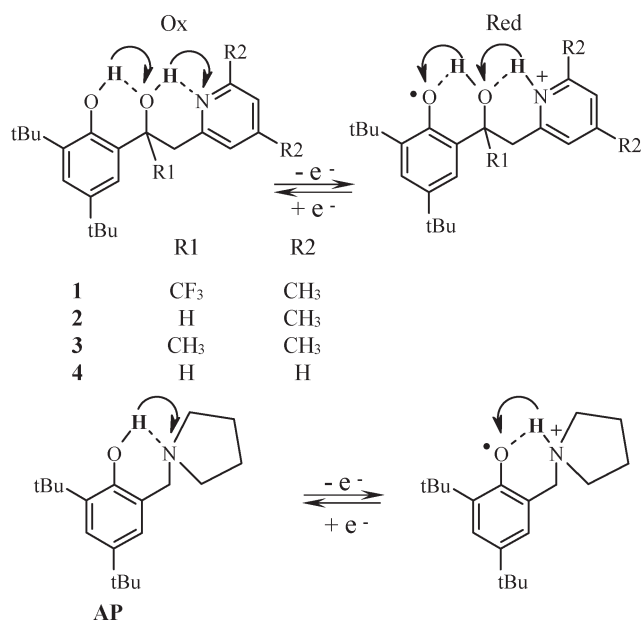
boosted by the necessity to face increasing energy challenges. Focusing on reactions where proton and electron transfers involve different sites,<sup>3</sup> particular emphasis has been put on the possibility that proton and electron transfer steps are concerted giving rise to CPET (concerted proton–electron transfer) reactions as opposed to stepwise pathways in which proton transfer precedes (PET) or follows (EPT) electron transfer as represented in Scheme 1 with the example of the oxidation of a phenol recalling the emblematic example of tyrosine<sub>Z</sub> in photosystem II (PSII).<sup>4</sup>

CPET pathways possess the advantage of circumventing the stepwise pathway high-energy intermediates, even though the thermodynamic benefit of going through the CPET pathway may have a kinetic counterpart.

Because it requires efficient proton tunneling, the occurrence of concerted processes implies short distances between the group generating the proton upon oxidation and the proton acceptor (and *vice versa* for a reduction process), which is usually accompanied by the formation of a hydrogen bond between the two groups. The distances over which the proton may travel as the result of a CPET reaction are therefore limited to the rather small values of H-bond length, in contrast with the electron in outersphere electron transfer reactions with no coupled proton transfer. The idea according to which this distance might be substantially increased by inserting a hydrogen-bond relay between the group being oxidized and the distant proton acceptor has recently been explored successfully.<sup>5,6</sup> The relay is an OH group, able to accept a H-bond from the moiety being oxidized and, at the same time, to form a H-bond with the proton accepting group, without going through a protonated state in the course of the reaction (Scheme 2).

Although these molecules are not as flexible as the water chains involved in Grothuss-type transport of protons, the OH group in these molecules does possess the basic

SCHEME 2



property of water molecules since it is both a hydrogen-bond acceptor and a hydrogen-bond donor. For these reasons, we bring together in the following discussion recent results pertaining to the dynamic oxidative response of molecules containing a H-bond relay on the one hand (first section of this Account) and to the oxidation of phenol with water (in water) as the proton acceptor on the other (second section).<sup>7</sup> Older electrochemical results relative to the reduction of superoxide ion in the presence of water will also be recalled (third section) so as to complete the picture of what is presently known on the concertedness of electron transfer with proton transport over simple H-bond relays and H-bond networks. The development of the discussion in this framework is also relevant to the role that water channels are supposed to play in various natural systems.<sup>8</sup> It is interesting in this regard to note the presence of water molecules possibly partaking in proton transport in the tyrosine<sub>Z</sub>–histidine<sub>190</sub>–OEC region of PSII, for which a CPET mechanism is admitted,<sup>9a</sup> as appears in a very recently published 1.9 Å-resolution structure (Figure 1).<sup>9b</sup>

## H-Bond Relays in Proton-Coupled Electron Transfers

The series of molecules containing an oxidizable phenol and a pyridine group that serves as proton acceptor and an alcohol function between them (Scheme 2) was synthesized in order to test the concept of H-bond relay. Their oxidation was investigated by means of cyclic voltammetry<sup>10,11</sup> and compared with the response obtained with a previously

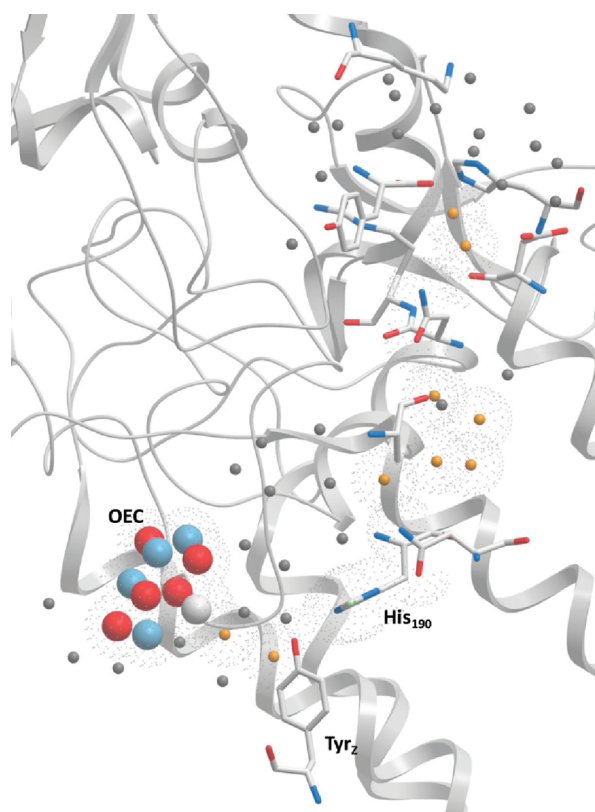


**FIGURE 1.** Structure around tyrosine<sub>z</sub> in PSII emphasizing the hydrogen bond pattern from the OEC to the luminal bulk phase, according to the 1.9 Å structure (PDB ID, 3ARC).<sup>9b</sup> Oxygen-evolving complex (OEC): blue spheres = Mn; white sphere = Ca; red spheres = O. Water molecules participating in the hydrogen-bond network are depicted in orange, whereas those not participating are depicted in dark gray. For the amino acids participating in the hydrogen-bond network, white sticks = C; red sticks = O; blue sticks = N.

investigated amino phenol (**AP** in Scheme 2) in which the proton generated by phenol oxidation travels directly to the amine in the absence of H-bond relay.<sup>12–14</sup>

The cyclic voltammetric traces (Figure 2) display partial chemical reversibility, the cathodic reverse trace corresponding to the re-reduction of the phenoxyl radical generated during the anodic scan as represented in Scheme 2.<sup>15</sup> The standard potential,  $E^0$ , of the O/R redox couple, is obtained as the midpoint between the anodic and cathodic peak potential (see Table 1).<sup>11</sup> The kinetics of this electrochemical electron transfer reaction can be derived from the distance between the anodic and cathodic peak, based on the Butler–Volmer equation:<sup>11</sup>

$$\frac{i}{FS} = k_s \exp\left[\frac{F}{2RT}(E - E^0)\right] \left\{ [\text{Red}] - \exp\left[-\frac{F}{RT}(E - E^0)\right] [\text{Ox}] \right\} \quad (1)$$

( $S$  = electrode surface area;  $[\text{Red}]$  and  $[\text{Ox}]$  are the concentrations of reduced and oxidized forms at the

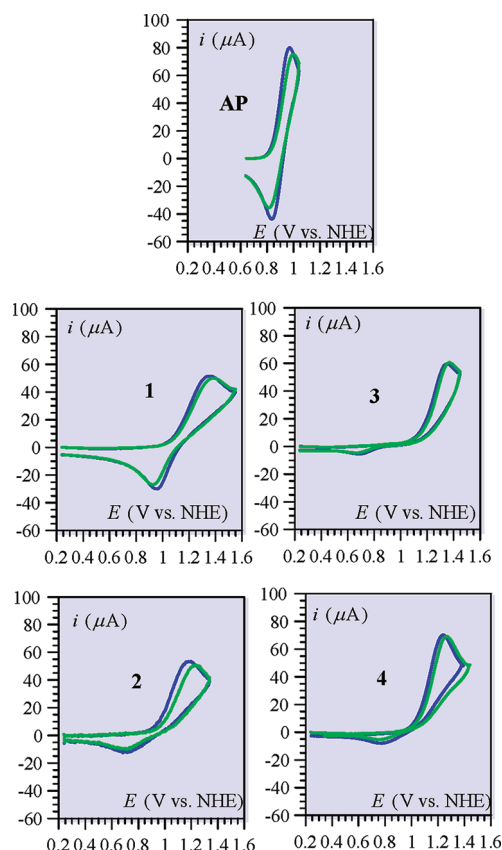


**FIGURE 2.** Cyclic voltammetry of the molecules shown in Scheme 2 in  $\text{CH}_3\text{CN} + 0.1 \text{ M Bu}_4\text{NBF}_4$ . Scan rate = 2 V/s, except for AP, which is 5 V/s.<sup>16</sup> Temp = 23 °C. Blue and green traces were taken in the presence of 1%  $\text{CH}_3\text{OH}$  or  $\text{CD}_3\text{OD}$ , respectively.

electrode surface;  $E$  = electrode potential). Equation 1 is a linear approximation<sup>11</sup> of the law relating the rate of the electrochemical reaction, represented by the current  $i$ , to the driving force of the reaction,  $F(E - E^0)$ . Equation 1 is the electrochemical equivalent of a linear kinetics vs thermodynamics free energy relationship in homogeneous chemistry with a symmetry factor of 1/2;  $k_s$  is the standard rate constant, that is, the rate constant at zero driving force (for  $E = E^0$ ). It is a measure of the intrinsic reactivity of the molecule toward oxidation. The values of  $k_s$  for the four H-bond relay molecules and for the reference amino-phenol are gathered in Table 1. Variations with temperature in the case of **1** led to an Arrhenius plot that may be described by eq 2:<sup>6</sup>

$$\ln k_s = \ln Z^{\text{het}} - \frac{1}{4RT} (\lambda + 2F\phi_s + 4\Delta Z\text{PE}^\ddagger - 2\Delta Z\text{PE}) \quad (2)$$

which allow the separation between the pre-exponential factor  $Z^{\text{het}}$ , given by the intercept and includes the

**TABLE 1.** Analysis of the Kinetics and Mechanism of the H-Bond-Relayed CPET Reaction<sup>a</sup>

cmp	AP	<b>1</b>	<b>2</b>	<b>3</b>	<b>4</b>
$E_{\text{H}}^{0b}$ ( $E_{\text{D}}^{0b}$ )	0.85	1.150 (1.143)	0.944 (0.957)	1.016 (1.010)	1.005 (1.010)
$k_{\text{S,H}}^{c,e}$ ( $k_{\text{S,D}}^{c,e}$ )	$8 \times 10^{-3}$	$9 \times 10^{-4}$ ( $6.3 \times 10^{-4}$ )	$4.5 \times 10^{-4}$ ( $2.7 \times 10^{-4}$ )	$8 \times 10^{-5}$ ( $4 \times 10^{-5}$ )	$4.5 \times 10^{-4}$ ( $3.1 \times 10^{-4}$ )
$\lambda_i^d$	0.390 (0.410)	0.405 (0.386)	0.433	0.420	0.443
$Z_{\text{H}}^{\text{het}}/Z_{\text{ref}}^f$	0.64	0.07	0.03	0.006	0.03
$(Z_{\text{D}}^{\text{het}}/Z_{\text{ref}}^f)$	(0.18)	(0.02)	(0.01)	(0.001)	(0.01)
$\text{KIE} = Z_{\text{H}}^{\text{het}}/Z_{\text{D}}^{\text{het}}^g$	3.4	2.9	3.4	4.1	2.9

<sup>a</sup>The subscripts H and D indicate that the measurements have been carried out at 23°C in the presence of 1% CH<sub>3</sub>OH or CD<sub>3</sub>OD, respectively. <sup>b</sup>Standard potentials in V vs NHE. <sup>c</sup>Standard rate constants (eq 1) in cm/s. <sup>d</sup>Intramolecular reorganization energy calculated from the energy of the starting molecule in the geometry of the distal radical cation (see Scheme 1); between parentheses, from the energy of the distal radical cation in the geometry of the starting molecule. <sup>e</sup>Error on  $k_{\text{S}}$  is 3%, based on a 3 mV uncertainty on the anodic-to-cathodic peak potential difference.  $Z_{\text{ref}} = 5.4 \times 10^4$  cm/s is the value expected for a simple electron transfer reaction. <sup>f</sup><sup>g</sup>Uncertainty 6%, that is, ca.  $\pm 0.2$ .

reorganization energy  $\lambda$  (i.e., the internal reorganization  $\lambda_i$  + the solvent reorganization  $\lambda_o$ ), obtained from the slope;  $\phi_{\text{S}}$  is the potential difference between the solution and the reaction site;  $\Delta Z_{\text{PE}}^{\ddagger}$  and  $\Delta Z_{\text{PE}}$  are the zero-point energies in the transition state and in the initial state, respectively (as appear in Figure 3). Equation 2 is the result of an analysis of electrochemical CPET reactions that derives from a double application of the Born–Oppenheimer approximation to electrons, protons, and heavy atoms of the system.<sup>17</sup> The transition state is defined toward the heavy atom reaction coordinate by the intersection of two parabolae in the Marcus–Hush–Levich way (blue curves in Figure 3).<sup>20–22</sup> At the transition state, the dependence of the potential energy toward the proton coordinates is depicted schematically in the upper inserts of Figure 3a,b, thus showing how electron transfer is concerted with proton tunneling. In the case of a H-bond relay, the variation of the potential energy at the transition state is a surface, function of the two coordinates,  $q_{\text{H}'}$ , and  $q_{\text{H}''}$ , along which the two protons tunnel, whereas with the aminophenol it takes the form of a curve, a function of the single coordinate  $q_{\text{H}}$ .

For **1**, the term  $\lambda + 2F\phi_{\text{S}} + 4\Delta Z_{\text{PE}}^{\ddagger} - 2\Delta Z_{\text{PE}} = 1.550$  eV is almost the same as for the aminophenol, **AP** (1.544 eV<sup>14</sup>). On top of this, quantum chemical estimates of  $\lambda_i$  showed that it is practically constant in the series, including **AP** (Table 1). Solvent reorganization and the other parameters are also expected to be similar among these compounds. It follows that the  $\lambda + 2F\phi_{\text{S}} + 4\Delta Z_{\text{PE}}^{\ddagger} - 2\Delta Z_{\text{PE}}$  term, and therefore  $\lambda$  is practically the same in the whole series, ca. 1.54 eV for proton transfer and ca. 1.47 eV for deuteron transfer as derived previously for the aminophenol. The values of  $Z^{\text{het}}$  then ensue by application of eq 2 for both the proton and deuteron transfer.  $Z^{\text{het}}$  is a combined

measure of the formation of precursor complexes over a range of significant reacting distances on one hand and of the efficiency of proton tunneling through the barrier shown in the upper insert of Figure 3, on the other. As for the aminophenol,<sup>14</sup> an estimate of the efficiency of proton tunneling is obtained by dividing the values thus obtained by the value of the pre-exponential factor that would have been obtained for a simple outersphere electron transfer under the same conditions ( $Z_{\text{ref}} = 5.4 \times 10^4$  cm/s).<sup>14</sup> The low values obtained for all H-bond relay molecules (Table 1) show that their CPET oxidations fall in the nonadiabatic regime in the whole series. The H/D kinetic isotope effect, designated by KIE, can then be obtained as the ratio  $\text{KIE} = Z_{\text{H}}^{\text{het}}/Z_{\text{D}}^{\text{het}}$  (Table 1). It is observed, as expected, that the largest KIE corresponds the lowest value of  $Z_{\text{H}}^{\text{het}}/Z_{\text{ref}}$  (and  $Z_{\text{D}}^{\text{het}}/Z_{\text{ref}}$ ), that is, to the most difficult proton (deuteron) tunneling, although the variations are small, just above the experimental uncertainty. Future development of the modeling of the KIE for these two-dimensional CPET reactions is clearly required.

It thus appears that reorganization parameters are not the main factors that make the CPET oxidation of the four H-bond relay molecules intrinsically slower than the oxidation of the aminophenol in which a single proton is moved concertedly with electron transfer, unlike what was hastily concluded from a preliminary analysis.<sup>5</sup> The reason that makes CPET oxidation of the four H-bond relay molecules intrinsically slower than the oxidation of the aminophenol is thus essentially related to the magnitude of the pre-exponential factor as appears in Table 1.<sup>6,23</sup> As expected, the efficiency of tunneling is less in the first case, where two protons are moved concertedly with electron transfer, than in the second where a single proton is transferred. The variations of the pre-exponential factor within the H-bond relay series is likely to result from the influence of the substituents of the alcohol on the balance between the

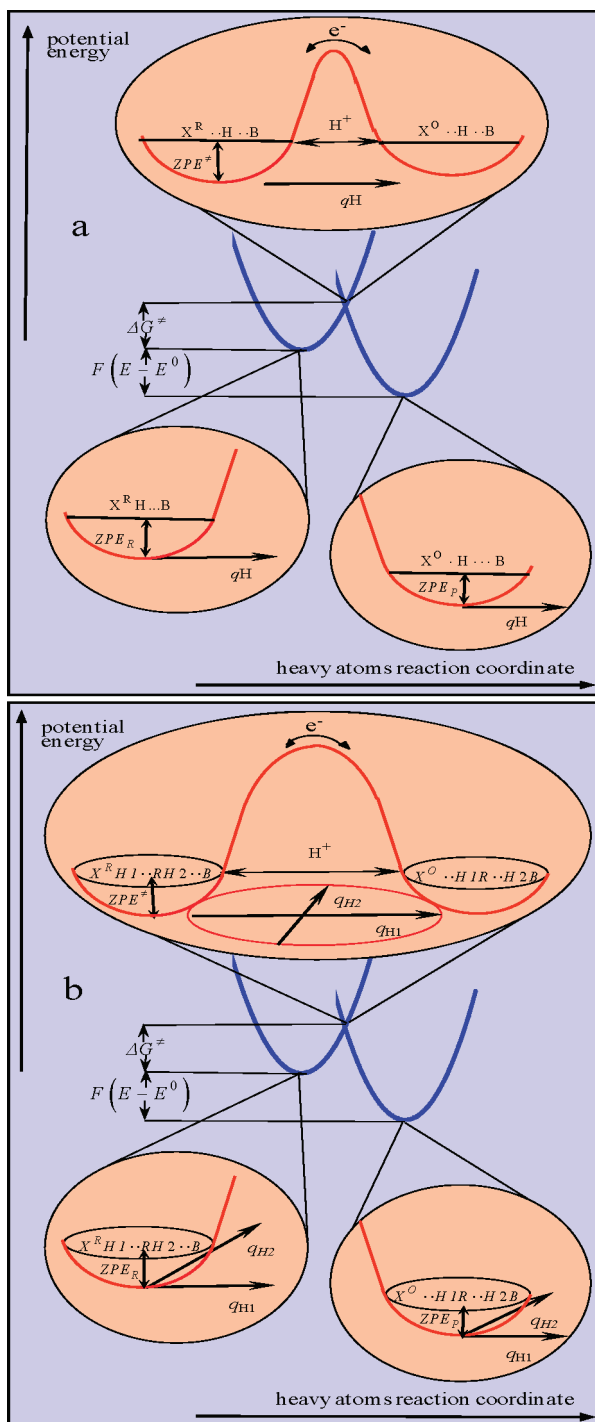
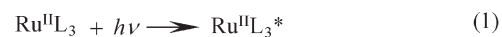


**FIGURE 3.** Potential energy curves for the reorganization of the heavy atoms of the system, including solvent molecules (blue parabolae), and for the proton displacement concerted with electron transfer (upper inserts). In the aminophenol case (a), the dependence of potential energy toward the proton coordinate takes the form of a curve. In the H-bond relay case (b), it has the form of a surface. The symbols are defined in Scheme 2 and in the text.

H-bond accepting and H-bond donating properties of the central OH group, inducing changes in the proton potential energy surface.

### SCHEME 3



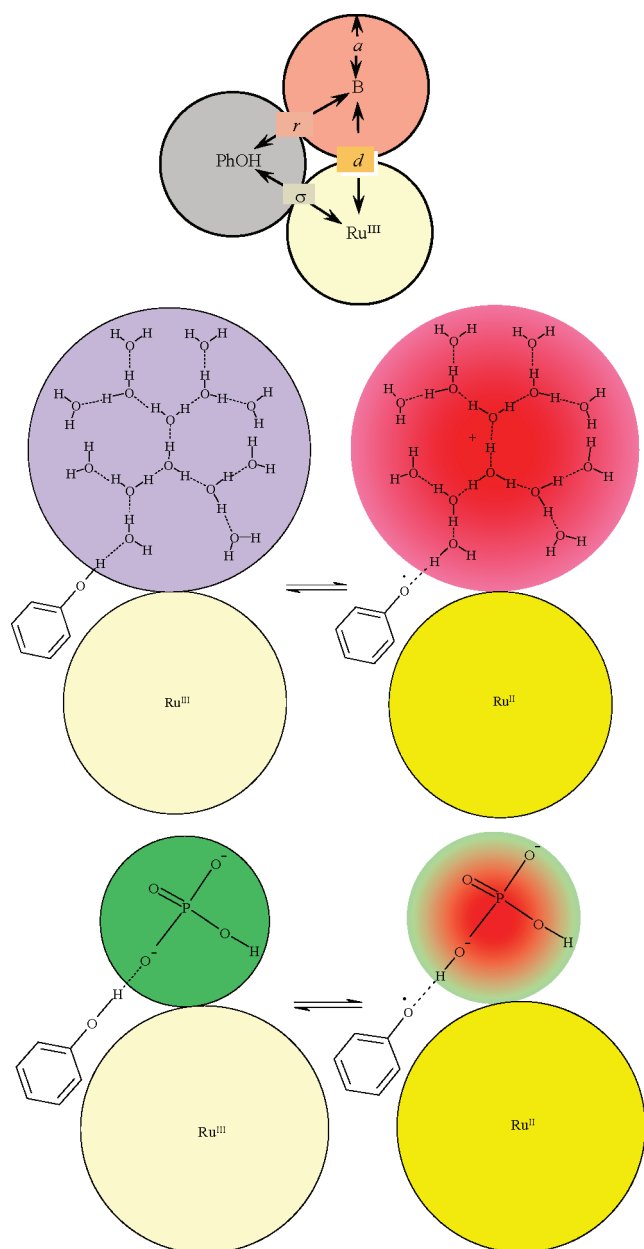
### Oxidation of Phenol with Water (in Water) as the Proton Acceptor

The preceding discussion has shown that a concerted proton–electron transfer reaction does take place when a H-bond relay is placed between the proton producing group and the proton acceptor, showing the compatibility of concerted proton–electron transfer with an extremely simplified Grotthuss-type transport mechanism, a “one-shot” Grotthuss mechanism. Is a concerted mechanism compatible also with a true Grotthuss proton transport when water, in water, is the proton acceptor is the question we address now. The illustrating reaction was the oxidation of a phenol as in the above discussion, although a flash photolysis method<sup>7,24</sup> was used instead of an electrochemical method. It consisted in generating the  $\text{Ru}^{\text{III}}\text{bpy}_3$  complex by quenching the corresponding photoexcited  $\text{Ru}^{\text{II}}$  complex by the methylviologen dication and monitoring the regeneration of the  $\text{Ru}^{\text{II}}$  ground state complex upon reaction of  $\text{Ru}^{\text{III}}\text{bpy}_3$  with phenol (Scheme 3). The reaction was first investigated in unbuffered water so as to establish the mechanism and kinetic characteristics of reaction 3 in Scheme 3. In order to emphasize the special behavior of water (in water), the reaction was contrasted with the reaction involving more usual proton acceptors (reaction 4 in Scheme 3) such as hydrogen phosphate and, more succinctly, pyridine.<sup>7,25</sup>

Mechanism analysis and determination of the kinetic characteristics rested on the variation of the rate constant with temperature in unbuffered media, using also the variations previously observed with the driving force of the reaction at a given temperature obtained by changing the electron acceptor.<sup>24</sup> The H/D kinetic isotope effect was an additional precious source of information.

The main results are summarized in Figure 4. In unbuffered water, the pseudo-second-order (water is the solvent) rate constant is the same at pH 2 and 4 over the whole range of temperature, whereas there is a definite increase of the rate constant when going to pH = 7.2. A  $\text{H}_2\text{O}$ –CPET pathway thus predominates at the first pH values, which increasingly enters in competition with an  $\text{OH}^-$ –PET pathway as the pH increases. Repeating these experiments in  $\text{D}_2\text{O}$  allows the

## SCHEME 4. Third-Order Reacting Clusters



determination of the H/D isotope effect characterizing the  $\text{H}_2\text{O}$ –CPET as a function of temperature (Figure 4b). The observation of a substantial H/D isotope effect confirms the concerted character of the reaction. We also note that it markedly decreases with temperature. With hydrogen phosphate as proton acceptor, the rate constant for the  $\text{PO}_4\text{H}^{2-}$ –CPET pathway is extracted from the raw data according to:

$$\begin{aligned} k_{\text{buf}, \text{pH}=7.2}^{\text{H}} &= k_{\text{H}_2\text{O}}^{\text{CPET}, \text{H}} + k_{\text{OH}^-}^{\text{PET}, \text{H}} + k_{\text{PO}_4\text{H}^{2-}}^{\text{CPET}, \text{H}} [\text{PO}_4\text{H}^{2-}] \\ &= k_{\text{unbuf}, \text{pH}=7.2}^{\text{H}} + k_{\text{PO}_4\text{H}^{2-}}^{\text{CPET}, \text{H}} [\text{PO}_4\text{H}^{2-}] \end{aligned}$$

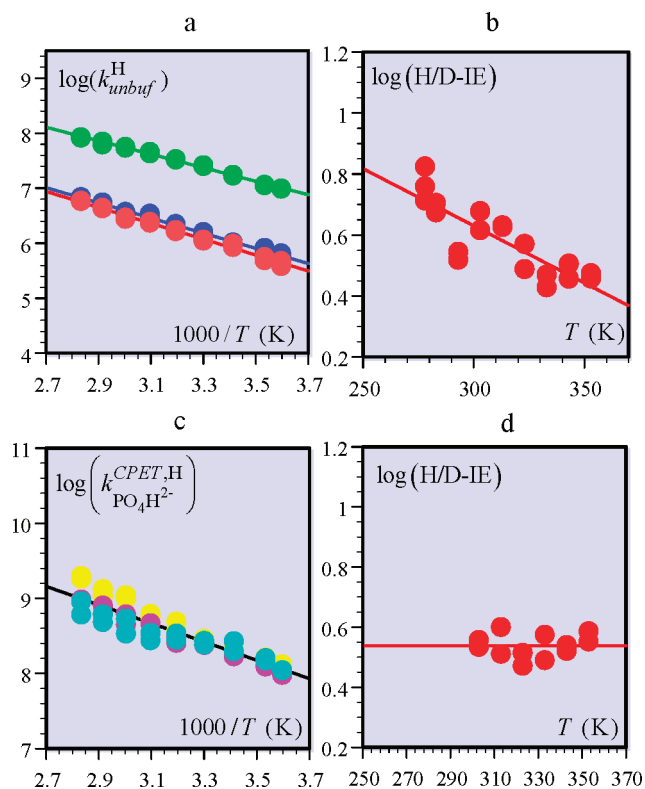


**FIGURE 4.** (a) Pseudo-second-order rate constant (in  $\text{M}^{-1} \text{s}^{-1}$ ) of the reaction of  $\text{Ru}^{\text{III}}(\text{bpy})_3$  with phenol in unbuffered media at pH = 2 (blue dots), 4 (red dots), or 7.2 (green dots) as a function of temperature. (b) Variation of the H/D isotope effect,  $\text{H/D-IE} = (k_{\text{unbuf}}^{\text{H}}/k_{\text{unbuf}}^{\text{D}})_{\text{pH}=2}$ , with temperature. (c) third-order rate constant (in  $\text{M}^{-2} \text{s}^{-1}$ ) for the reaction with hydrogen phosphate (from the variations of the second-order experimental rate constant with hydrogen phosphate concentration: 0.1 (yellow), 0.5 (magenta), 1 M (cyan)). (d) H/D isotope effect,  $\text{H/D-IE} = k_{\text{PO}_4\text{H}^{2-}}^{\text{CPET}, \text{H}}/k_{\text{PO}_4\text{H}^{2-}}^{\text{CPET}, \text{D}}$ , as a function of temperature.

The variation of this third-order rate constant with temperature is shown under the form of an Arrhenius plot in Figure 4c. It is noteworthy that the H/D isotope effect does not vary with temperature in this case (Figure 4d).

It appears that the rate constant in the case of hydrogen phosphate is much larger than that with water, by ca. 2 orders of magnitude, just because the driving force of the reaction is much larger in the first case than in the second, by ca. 0.42 eV at 25 °C. What is of interest for the present discussion is not the comparison of the absolute reactivities but the comparison of the intrinsic reactivities, that is, the reactivities at zero driving force, as a tool to understand how Grotthuss-type mechanisms may be involved in proton-coupled electron transfers when water (in water) is the proton acceptor. Analysis of the experimental results was based on a model whose main features, summarized in Figure 3a, derive from a double application of the Born–Oppenheimer approximation as discussed in the preceding

**TABLE 2.** Kinetics Parameters of the H<sub>2</sub>O–CPET and PO<sub>4</sub>H<sup>2-</sup>–CPET Oxidation of Phenol<sup>a</sup>

Parameters	H <sub>2</sub> O	PO <sub>4</sub> H <sup>2-</sup>
$\lambda$ ( $= \frac{\lambda_{\text{ox}} + \lambda_{\text{CPET}}}{2}$ ) <sup>b</sup>	0.51 ± 0.02	0.72 ± 0.02
$\lambda_{\text{CPET}}$ (eV)	0.45 ± 0.04	0.86 ± 0.04
$2R \frac{\beta^2}{f}$ (K <sup>-1</sup> )	0.0125 (H) 0.020 (D) ± 0.001	0 (H) 0.0064 (D) ± 0.001
$\ln Z_{\text{eq}} = \ln \left\{ \left[ 4\pi N_A \sigma^2 \sqrt{(\delta\sigma^2)} \sqrt{\pi/2} \right]^b \times \left[ 4\pi N_A r^2 \sqrt{\frac{RT}{f}} \sqrt{\pi/2} \right] \times \left[ \frac{2}{\sqrt{\lambda}} \left( \frac{\pi}{RT} \right)^{\frac{3}{2}} C_{\text{eq}}^2 v_n \right] \right\}$	19.5 (H) ± 0.6  15.9 (D) ± 0.6	16.8 (H) ± 0.6  14.8 (D) ± 0.6

<sup>a</sup> $\lambda_{\text{ox}} = 0.57$  eV: self-exchange reorganization energy for the Ru<sup>III/II</sup> couple.<sup>27</sup> <sup>b</sup>For the definition of  $\sigma$  and  $r$ , see top of Scheme 4.  $(\delta\sigma^2)^{1/2}$  = amplitude of the variation of  $\sigma$ ;  $f$  = force constant of the harmonic oscillator of the H-bond between PhOH and B;  $C_{\text{eq}}$  = coupling constant between the two electronic states in the transition state at equilibrium distance between PhOH and B;  $v_n$  = nuclear frequency.  $\beta$  is the attenuation factor of the exponential decay of the vibronic coupling of the two states with distance.

section. The transition state is located at the crossing of the potential energy profiles toward the heavy-atom coordinate of the reactant and product systems (parabola in Figure 3a), leading to the following Marcus-type expression of the rate constant:

$$k = Z \exp \left[ -\frac{W_R}{RT} \right] \exp \left[ -\frac{\lambda}{4RT} \left( 1 + \frac{\Delta G^0 - W_R + W_P}{\lambda} \right)^2 \right] \quad (3)$$

The pre-exponential factor,  $Z$ , is obtained from the termolecular pre-exponential factor,  $Z_{\text{ter}}$ , as  $Z = Z_{\text{ter}}[\text{B}]$ , where in the case of water,  $[\text{B}] = 1$  M is the activity of water in water and  $Z_{\text{ter}}$  is the pre-exponential factor of the reverse reaction,  $\text{ArO}^* + \text{Ru}^{\text{II}} + \text{H}^+$ . In the case of hydrogen phosphate,  $[\text{B}] = 1$  M and  $Z_{\text{ter}}$  is the pre-exponential factor of the direct reaction as well as the reverse reaction.  $Z_{\text{ter}}$  is a combined measure of the formation of precursor complexes over a range of significant reacting distances and of the efficiency of proton tunneling through the barrier shown in the upper insert of Figure 3c. It may be expressed by eq 4:<sup>26</sup>

$$Z_{\text{ter}} = Z_{\text{eq}} \exp \left( \frac{2RT\beta^2}{f} \right) \quad (4)$$

which involves the combination of two intrinsic parameters: an equilibrium pre-exponential factor  $Z_{\text{eq}}$ , characterizing the coupling of electronic states in the transition state at equilibrium distance (Figure 3a) and a distance-sensitivity parameter  $\beta^2/f$  in which  $\beta$  is the attenuation factor of the exponential decay of the

vibronic coupling of the two states with distance and  $f$  is the force constant of the harmonic oscillator of the H-bond between PhOH and the proton acceptor B.

In the Franck–Condon exponential term of eq 3,  $\lambda$  is the reorganization energy,  $\Delta G^0$  is the reaction standard free energy, and  $W_R$  and  $W_P$  are the work terms required to bring the reactants and products respectively, from infinite separation to reacting distance. The Arrhenius plots shown in Figures 4a,c result from the linearization of eq 3 over the experimental temperature range, leading to expressions of the intercept and slope that contain three terms, related, respectively, to an intrinsic kinetic parameter, to a thermodynamical effect, and to a distance-sensitivity parameter. In the case of water, the three parameters,  $\lambda$ ,  $Z_{\text{eq}}$ , and  $\beta^2/f$  were then obtained from the Arrhenius slope and intercept (Figure 4a), which provide two relationships between these three parameters, while a third relationship is derived from the variations of the rate constant with the driving force using the previously reported data.<sup>24</sup> The resulting values of the three parameters are reported in Table 2 (for details, see ref 7).

It is remarkable that the reorganization energy in the case of water as proton acceptor is much smaller than in the case of hydrogen phosphate. Going on the analysis requires separating reorganization for CPET oxidation of phenol from reorganization for the corresponding reduction of the oxidant partner, Ru<sup>III</sup>(bpy)<sub>3</sub>, according to

$$\lambda = \frac{\lambda_{\text{ox}} + \lambda_{\text{CPET}}}{2}$$

where the overall reorganization energy,  $\lambda$ , is split into two contributions, as in the case of outersphere electron transfer,<sup>20</sup>  $\lambda_{\text{ox}}$ , relative to Ru<sup>III</sup>(bpy)<sub>3</sub> self-exchange  $\text{Ru}^{\text{II}} + \text{Ru}^{\text{III}} \rightleftharpoons \text{Ru}^{\text{III}} + \text{Ru}^{\text{II}}$ , and  $\lambda_{\text{CPET}}$ , relative to the CPET self-exchange  $(\text{ArOH} \cdots \text{B}) + (\text{ArO}^* \cdots \text{HB}) \rightleftharpoons (\text{ArO}^* \cdots \text{HB}) + (\text{ArOH} \cdots \text{B})$ .

The major part of this reorganization energy may be ascribed to solvent reorganization induced by the generation of a water-solvated proton. The ensuing value of the reorganization energy, 0.45 eV, is remarkably small, much smaller than the value found for hydrogen phosphate. This indicates that the proton charge is not concentrated on a single hydrogen atom or even on a single protonated water molecule. A rough estimate of the solvation radius of this water cluster may be obtained from<sup>7</sup>

$$\lambda_0(\text{eV}) \cong \frac{3}{a(\text{\AA})}$$

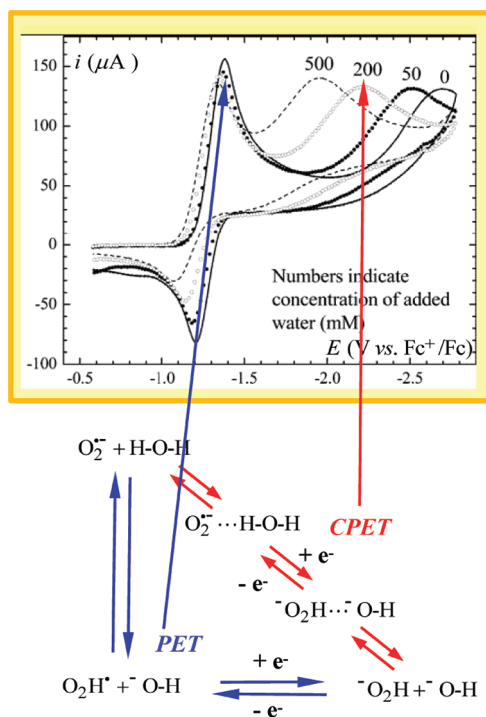


**FIGURE 5.** Cyclic voltammetry of the reduction of dioxygen in dimethylformamide (+ 0.1 M  $\text{NBu}_4\text{BF}_4$ ) at a glassy carbon electrode at 0.2 V/s in the presence of increasing  $\text{H}_2\text{O}$  concentrations (numbers on each curve in mM). Add 0.645 V to obtain a potential scale referred to the NHE.

leading to a value of 6.5 Å (Scheme 4), compatible with recent spectroscopic observations.<sup>28</sup> It is also in agreement with the conclusions of a current study of the reduction of dioxygen in concentrated acid solutions where the proton plays the converse role of a reactant.<sup>29</sup> The proton acceptor is therefore not a single water molecule but a cluster containing many water molecules indicating that the CPET process involves the concerted, although not necessarily synchronous, displacement of several protons in agreement with recent findings concerning photochemically triggered proton transfer.<sup>30</sup> If proton displacements were occurring sequentially, the first of these would involve strong localization of the proton charge inconsistently with the small value of the reorganization energy found experimentally.

The equilibrium pre-exponential factor,  $Z_{\text{eq}}$ , featuring the electronic states coupling from the precursor complex at its equilibrium distance, is larger in the case of water ( $3 \times 10^8 \text{ M}^{-2} \text{ s}^{-1}$ ) than in the case of hydrogen phosphate ( $2 \times 10^7 \text{ M}^{-2} \text{ s}^{-1}$ ), indicating that proton translocation, concerted with electron transfer, is more efficient in water than a CPET process where the proton is more localized.

The significant variation of the H/D isotope effect with temperature (Figure 4b) provides additional mechanistic insights. The variation of the H/D isotope effect (Figure 4b) leads to the values of  $2R(\beta_{\text{D}}^2/f)$  and  $Z_{\text{eq,D}}$  reported in Table 2 together with their  $\text{H}_2\text{O}$  counterparts, after account has been taken of the variations of the free energy of the reaction with temperature, which gives rise to a modest thermodynamic effect. As expected, the equilibrium pre-exponential factor  $Z_{\text{eq}}$  characterizing the coupling of electronic states in the transition state at equilibrium distance is smaller with deuterium than with hydrogen and the distance-sensitivity parameter  $\beta^2/f$  is larger in agreement with the occurrence of a Grotthuss-type mechanism during the CPET process. Additional evidence is provided by comparison with hydrogen phosphate. In this case, Arrhenius plots (Figure 4c) can only be fitted by means of vanishingly small values of  $\beta^2/f$  and the resulting reorganization energy, 0.86 eV, is much larger than that with water. The solvation radius, ca. 3.5 Å (Scheme 4) is accordingly much smaller, being close to a quantum calculated value,<sup>7</sup> in agreement with the assumption that the reorganization energy is essentially due to solvent reorganization in the case of hydrogen phosphate too.

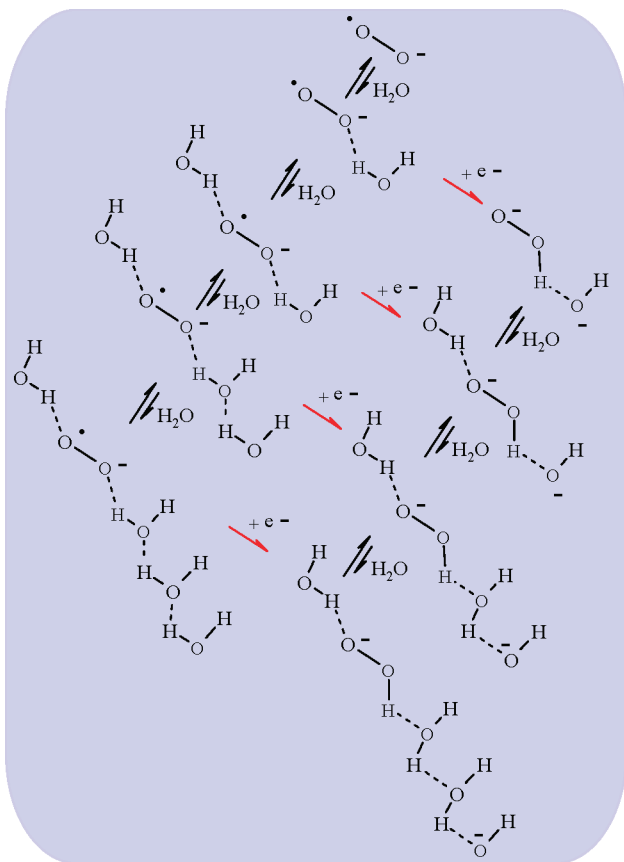
In total, hydrogen phosphate gives rise to a much “stiffer” proton acceptor system than does water (in water), in line, in the latter case with a Grotthuss-type proton transport associated with the CPET reaction. Pyridine shows a behavior similar to hydrogen phosphate, albeit a few water molecules appear to be associated with the pyridine moiety in the delocalization of the proton charge.<sup>25</sup>

### Reduction of Superoxide Ion with Water as the Proton Donor

The reduction of superoxide ion,  $\text{O}_2^-$ , provides an early example of the special character of water as proton acceptor in CPET reactions.<sup>31</sup> In an aprotic solvent, such as dimethylformamide, dioxygen shows an almost reversible cyclic voltammetric first wave (Figure 5). The second thick and irreversible wave corresponds to the reduction of the superoxide ion produced at the first wave. Its location is heavily dependent on the concentration of water introduced into the solution.<sup>32,33</sup> The partial irreversibility of the first wave corresponds to the proton-coupled electron transfer to superoxide yielding the  $\text{HO}_2^-$  ion according to a PET mechanism (blue arrows in Figure 5). At the second wave, a CPET reaction takes place (red arrows in Figure 5). The huge sensitivity of the location of the second wave to the addition of water indicates, after all other mechanistic explanations have been ruled out, that a concerted transfer of one



SCHEME 5



electron and one proton through short water chains takes place (Scheme 5). It is indeed thermodynamically favored by a decrease of the attending repulsion between  $\text{HO}_2^-$  and  $\text{OH}^-$  even though there might be some kinetic counterpart to this advantage. The observed increase of the H/D kinetic effect on superoxide reduction with concentration of added water confirms this mechanism assignment reflecting the increase of the  $\text{H}^+$  tunneling distance.

## Conclusions and Prospects

Proton–electron transfer reactions are of great importance in natural and synthetic processes, particularly those involved in the resolution of modern energy challenges. In this framework, concerted proton–electron transfers, as opposed to stepwise pathways, are of particular significance since they may bypass the high-energy intermediates of the stepwise pathways, even though this thermodynamic benefit may have a kinetic cost. The concerted character of the reaction implies that the distance between the proton-generating site and the acceptor is short, of the order of the length of a H-bond. The various examples discussed in this Account show that this distance may be largely increased by

means of H-bond relays, possibly forming a H-bond network, positioned between the proton-producing and proton-accepting sites. The simplest systems illustrating this possibility consisted in inserting an alcohol group between a phenol function oxidation of which produces a proton and an amine proton receptor. Such an increase of the range of proton transport in a reaction where it is concerted with electron transfer is likewise observed in the simple oxidation of phenol with water as the proton acceptor in water as solvent. Electron transfer is then concerted with a Grotthuss-type transport, the charge of the released proton being delocalized over a large water cluster of ca. 7 Å equivalent radius. This means that the proton is released at an average distance of ca. 7 Å from the site where it has been generated.

The huge acceleration of the reduction of superoxide ion triggered by addition of water also implies the interference of water chains along which proton transport is similarly concerted with electron transfer. In the first of these systems, the positioning of the H-bond relay on a rigid molecular framework led to some slowing of the concerted pathway, more than in the case of the more flexible water H-bond network. In all cases the reaction remains remarkably fast, making, as far as concerted proton–electron transfers are concerned, the “H-bond” a bullet train. We hope that these few remarks will contribute to the understanding of the role of water chains or networks in proton transport concerted with electron transfer in natural systems, possibly with the help of purposely designed mimics.

*Dr. Cyril Louault and Mathilde Routier are thanked for their participation to the work described in this Account. Partial financial support from ANR (Grants ANR-07-BLAN-0280 and ANR-10-BLAN-0808) is gratefully acknowledged.*

## BIOGRAPHICAL INFORMATION

**Julien Bonin** received his Ph.D. in Physical Chemistry from the Université Paris-Sud XI in 2005. He then joined the Radiation Laboratory at the University of Notre Dame as a Postdoctoral Research Associate. Since 2006, he has been Associate Professor of Chemistry at the Université Paris Diderot, and he was a Visiting Scientist at the Chemistry Department of MIT during the spring of 2010. His current research interests include photo-induced electron transfers, proton-coupled electron transfers, and photocatalysis.

**Cyrille Costentin** received his undergraduate education at Ecole Normale Supérieure in Cachan and pursued his graduate studies under the guidance of Profs. Jean-Michel Savéant and Philippe Hapiot at the University Paris Diderot (Paris 7), where he received his Ph.D. in 2000. After one year as a postdoctoral fellow at the

University of Rochester, working with Prof. J. P. Dinnocenzo, he joined the faculty at the University of Paris Diderot as associate professor. He was promoted to professor in 2007. His interests include mechanisms and reactivity in electron transfer chemistry with particular recent emphasis on electrochemical and theoretical approaches to proton-coupled electron transfer processes.

**Marc Robert** was educated at the Ecole Normale Supérieure in Cachan, France, and obtained his Ph.D. in 1995 at the Paris Diderot University (Paris 7) under the supervision of Claude P. Andrieux and Jean-Michel Savéant. After one year as a postdoctoral fellow at The Ohio State University, working alongside Matt Platz, he joined the faculty at Paris Diderot University as associate professor. He was promoted to professor in 2004 and has been a member of the University Institute of France since 2007. His interests include electrochemical, photochemical, and theoretical approaches to electron transfer reactions, as well as proton-coupled electron transfer processes in both organic chemistry and biochemistry.

**Jean-Michel Savéant** received his education in the Ecole Normale Supérieure in Paris, where he became the Vice-Director of the Chemistry Department before moving to the University Paris Diderot (Paris 7) as a Professor in 1971. He has been Directeur de Recherche au Centre National de la Recherche Scientifique in the same university since 1985. In 1988–1989, he was a visiting professor at the California Institute of Technology. His current research interests involve all aspects of molecular and biomolecular electrochemistry as well as mechanisms and reactivity in electron transfer chemistry and biochemistry. Jean-Michel Savéant is a Member of the French Academy of Sciences and a Foreign Associate of the National Academy of Sciences of the United States of America.

**Cédric Tard** studied chemistry at the University of Paris-Sud and earned his Ph.D. degree in 2005 at the John Innes Centre (Norwich, U.K.) under the guidance of Prof. Chris Pickett. After two years as a postdoctoral fellow at the École Polytechnique (Palaiseau, France), he is currently working as a CNRS associate scientist at the University Paris Diderot. His research interests are centered on the synthesis of bioinspired molecules for electrochemical studies of proton-coupled electron transfer mechanisms.

#### FOOTNOTES

\*To whom correspondence should be addressed. E-mail: saveant@univ-paris-diderot.fr.

#### REFERENCES

- Nocera, D. G. Chemistry of Personalized Solar Energy. *Inorg. Chem.* **2009**, *48*, 10001–10017.
- Artificial Photosynthesis and Solar Fuels. Special Issue. *Acc. Chem. Res.* **2009**, *42*, 1859–2029.
- In contrast with H-atom transfer reactions.
- Proton-Coupled Electron Transfer. Thematic Issue. *Chem. Rev.* **2010**, *110*, 6937–7100.
- Costentin, C.; Robert, M.; Savéant, J.-M.; Tard, C. Inserting a Hydrogen-Bond Relay between Proton Exchanging Sites in Proton-Coupled Electron Transfers. *Angew. Chem., Int. Ed.* **2010**, *49*, 3803–3806.
- Costentin, C.; Robert, M.; Savéant, J.-M.; Tard, C. H-Bond Relays in Proton-Coupled Electron Transfers. Oxidation of a Phenol Concerted with Proton Transport to a Distal Base through an OH Relay. *Phys. Chem. Chem. Phys.* **2011**, *13*, 5353–5358.
- Bonin, J.; Costentin, C.; Louault, C.; Robert, M.; Savéant, J.-M. Water (in Water) as an Intrinsically Efficient Proton Acceptor in Concerted Proton Electron Transfers. *J. Am. Chem. Soc.* **2011**, *133*, 6668–6674.
- Wraight, C. A. Chance and Design-Proton Transfer in Water, Channels and Bioenergetic Proteins. *Biochim. Biophys. Acta, Bioenerg.* **2006**, *1757*, 886–912.
- (a) Hammarström, L.; Styring, S. Proton-coupled electron transfer of tyrosines in Photosystem II and model systems for artificial photosynthesis. The role of a redox-active link between catalyst and photosensitizer. *Energy Environ. Sci.* **2011**, *4*, 2379–2388. (b) Umena, Y.; Kawakami, K.; Shen, J.-R.; Kamiya, N. Crystal Structure of Oxygen-Evolving Photosystem II at a Resolution of 1.9 Å. *Nature* **2011**, *473*, 55–60.
- Cyclic voltammetry consists of monitoring the current resulting from isosceles triangular scanning of the electrode potential. Mechanism and kinetic analysis is based on the shape, height, and potential location of the resulting current–potential responses and their variation with parameters such as scan rate and reactant concentrations. For an introduction to this technique, see ref 11.
- Savéant, J.-M. *Elements of Molecular and Biomolecular Electrochemistry*; Wiley-Interscience: New York, 2006.
- Costentin, C.; Robert, M.; Saveant, J.-M. Electrochemical and Homogeneous Proton-Coupled Electron Transfers: Concerted Pathways in the One-Electron Oxidation of a Phenol Coupled with an Intramolecular Amine-Driven Proton Transfer. *J. Am. Chem. Soc.* **2006**, *128*, 4552–4553.
- Costentin, C.; Robert, M.; Savéant, J.-M. Adiabatic and Non-adiabatic Concerted Proton-Electron Transfers. Temperature Effects in the Oxidation of Intramolecularly Hydrogen-Bonded Phenols. *J. Am. Chem. Soc.* **2007**, *129*, 9953–9963.
- Costentin, C.; Robert, M.; Savéant, J.-M. Reorganization Energies and Pre-Exponential Factors in the One-Electron Electrochemical and Homogeneous Oxidation of Phenols Coupled with an Intramolecular Amine-Driven Proton Transfer. *Phys. Chem. Chem. Phys.* **2010**, *12*, 13061–13069.
- The partial lack of reversibility is presumably due to deprotonation of the radical cation, possibly involving traces of residual bases in the reaction medium.
- Since electron transfer is faster with AP than with 1–4, a larger scan rate is required to move away from a pure diffusion control of the current and to make electron transfer interfere significantly in the cyclic voltammetric response.
- Costentin, C.; Robert, M.; Savéant, J.-M. Electrochemical Concerted Proton and Electron Transfers. Potential-Dependent Rate Constant, Reorganization Factors, Proton Tunneling and Isotope Effects. *J. Electroanal. Chem.* **2006**, *588*, 197–206.
- Costentin, C.; Robert, M.; Savéant, J.-M. Concerted Proton–Electron Transfers: Electrochemical and Related Approaches. *Acc. Chem. Res.* **2010**, *43*, 1019–1029.
- Hammes-Schiffer, S. Theory of Proton-Coupled Electron Transfer in Energy Conversion Processes. *Acc. Chem. Res.* **2009**, *42*, 1881–1889.
- Marcus, R. A. Electron Transfer at Electrodes and in Solution - Comparison of Theory and Experiment. *Electrochim. Acta* **1968**, *13*, 995–1004.
- Hush, N. S. Homogeneous and Heterogeneous Optical and Thermal Electron Transfer. *Electrochim. Acta* **1968**, *13*, 1005–1023.
- Levich, V. G. In *Present State of the Theory of Oxidation-Reduction in Solution (Bulk and Electrode Reactions)* Delahay, P., Tobias, C. W., Eds.; Advances in Electrochemistry and Electrochemical Engineering; Wiley: New York, 1955, pp 250–371.
- In line with a recent theoretical study: Auer, B.; Fernandez, L. E.; Hammes-Schiffer, S. Theoretical Analysis of Proton Relays in Electrochemical Proton-Coupled Electron Transfer. *J. Am. Chem. Soc.* **2011**, *133*, 8282–8292.
- Bonin, J.; Costentin, C.; Louault, C.; Robert, M.; Routier, M.; Savéant, J.-M. Intrinsic Reactivity and Driving Force Dependence in Concerted Proton-Electron Transfers to Water Illustrated by Phenol Oxidation. *Proc. Natl. Acad. Sci. U.S.A.* **2010**, *107*, 3367–3372.
- Bonin, J.; Costentin, C.; Robert, M.; Savéant, J.-M. Pyridine as Proton Acceptor in the Concerted Proton Electron Transfer Oxidation of Phenol. *Org. Biomol. Chem.* **2011**, *9*, 4064–4069.
- Soudackov, A.; Hatcher, E.; Hammes-Schiffer, S. Quantum and Dynamical Effects of Proton Donor-Acceptor Vibrational Motion in Nonadiabatic Proton-Coupled Electron Transfer Reactions. *J. Chem. Phys.* **2005**, *122*, No. 014505.
- Sutin, N.; Brunschwig, B. S. Electron Transfer in Weakly Interacting Systems. *ACS Symp. Ser.* **1982**, *198*, 5–135.
- Stoyanov, E. S.; Stoyanova, I. V.; Reed, C. A. The Structure of the Hydrogen Ion (H<sub>aq</sub><sup>+</sup>) in Water. *J. Am. Chem. Soc.* **2010**, *132*, 1484–1485.
- Snir, O.; Wang, Y.; Tuckerman, M. E.; Geletii, Y. V.; Weinstock, I. A. Concerted Proton-Electron Transfer to Dioxygen in Water. *J. Am. Chem. Soc.* **2010**, *132*, 11678–11691.
- Cox, M. J.; Timmer, R. L. A.; Bakker, H. J.; Park, S.; Agmon, N. Distance-Dependent Proton Transfer along Water Wires Connecting Acid-Base Pairs. *J. Phys. Chem. A* **2009**, *113*, 6599–6606.
- Savéant, J.-M. Electrochemical Concerted Proton and Electron Transfers. Further Insights in the Reduction Mechanism of Superoxide Ion in the Presence of Water and Other Weak Acids. *J. Phys. Chem. C* **2007**, *111*, 2819–2822.